The Effect of Micro Turbulence
on Quartz Flotation Rate

Shahbazi, Behzad*+

Mining Engineering Department, Tarbiat Modares University, Tehran, I.R. IRAN

Rezai, Bahram

Mining Engineering Department, Amirkabir University of Technology, Tehran, I.R. IRAN

ABSTRACT: *In this research, the effect of micro turbulence on the flotation rate of quartz particles was investigated. The maximum particle Reynolds number (Re_p) was obtained at 60.25 with a particle size of -500+420 μm, impeller speed of 900 rpm, bubble surface area flux of 10.21 1/s and micro scale turbulence size of 162 μm. When the micro turbulence size was equal to the particle size, the maximum flotation rate of coarse particles ($Re_p>10$) was obtained at 1.47 1/min.*

KEY WORDS: *Flotation, Kinetics, Bubble, Input power, Turbulence.*

INTRODUCTION

Recent studies have suggested that the pulp (or collection) zone rate constant, k, is linearly dependent on the bubble surface area flux, S_b [1-3]. Where $S_b=6J_g/d_{32}$, J_g is the superficial gas rate and d_{32} is the Sauter mean diameter of the bubble. The relationship is usually expressed as $k=\alpha R_f S_b$, where α is the "floatability factor" which encompasses the contribution of particle size and hydrophobicity [4] and R_f is froth recovery factor which is defined as the ratio of the overall rate constant and he collection zone rate constant [5].

Based on an operating aspect, the impeller peripheral speed (N_s) provides an opportunity to control the specific input power (P) to the flotation cell slurry. Recent studies have highlighted the importance of local turbulent energy dissipation (ε) on both the frequency of bubble–particle collision and stability efficiency of the particle-bubble aggregate [6-8].

The turbulence plays a decisive part in the flotation process because it is responsible for collisions between particles and bubbles, i.e., the formation of aggregates as well as for the stability of the aggregates in the greater part of the machine volume [9]. Particles with kinetic energy greater than the detaching energy cannot float. Hence, for a given energy of the system and particle density, a maximum particle size for floatability can be expected. On the other hand, in keeping with the concepts discussed above there must be a maximum energy input in the pulp for there to be any collision formation. If the kinetic energy of the particles is lower than that required for collision formation, the particle may not float. Thus, for a given energy of the system and particle density, it can also be supposed that a lower grain size limit exists. Moreover, the upper limit is dependent on the maximum bubble-particle aggregate buoyancy and hence on the particle size. Since in the turbulent field this is, in turn, dependant on the dissipated energy, a direct relationship

remains between kinetic energy and floatability [10]. So far, the effect of hydrodynamic parameters on the flotation response of coarse and fine particles has been widely investigated [11-21]. The effect of input power and micro turbulence on the $k-S_b$ relationship has not been investigated thus far. So, in this research, the effect of input power and micro turbulence on the $k-S_b$ relationship is investigated using quartz particles.

EXPERIMETAL SECTION

Flotation tests were carried out in a mechanical laboratory flotation cell. An impeller diameter of 0.07 meters was used for pulp agitation and a cell with a square section was used in which the length and height were 0.13 and 0.12 meters, respectively. Impeller rotating speed was 900, 1000, 1100 and 1200 rpm and air flow rate was 60, 120, 180 and 240 l/h. Quartz particles (specific gravity=2.65 g/cm^3) of eight size classes containing -37, -53+37, -75+53, -106+75, -212+106, -300+212, -420+300 and -500+420 μm were used for flotation experiments. The frother was MIBC (methyl iso-butyl carbinol) with concentration of 22.4 ppm and C=2×CCC (CCC, critical coalescence concentration). The flotation experiments were carried out by dodecylamine collector (50 g/t) at a natural pH of 8.5 using local tap water. When S_b values were set, all the size fractions floated together under those exact conditions (Table 1). $K=\alpha R_f S_b$ is not universally accepted and certainly can only be valid up to a certain S_b (a limit on the S_b before the cell boils). So, in this investigation, S_b was 10.21 to 34.2 1/s. Also, in all experiments, the froth depth was shallow and froth recovery factor (R_f) was assumed equal to 1.

The air flow rate and impeller speed were set and the float product was collected at time intervals of 1, 2, 3 and 5 minutes. The recovery, R, determined as a function of time, t, and flotation rate constant was calculated. The batch wise flotation of mineral particles may be described by a first order rate equation where the removal rate of particles is given by:

$$\frac{dC}{dt} = -kC \tag{1}$$

Where C is the particle concentration in mass per unit volume and k is a 'rate constant'. The flotation rate constant was calculated assuming the first order rate equation for a batch cell, $R=R^*(1-\exp(-kt))$, and plotting $\ln(R^*-R/R^*)$ versus t. where R^* is infinite recovery (Fig. 1).

According to Fig. 1a, flotation recovery after 5 minutes was close to R^* approximately.

The bubble size distribution was measured in a device similar to the McGill bubble viewer. It consisted of a sampling tube attached to a viewing chamber with a window inclined at 15° from the vertical. The closed assembly was filled with water of a similar nature to that in the flotation cell (to limit changes in the bubble environment during sampling) and the tube was immersed in the desired location below the froth. Bubbles rose into the viewing chamber and were imaged by a digital camera as they slid up the inclined window, which was illuminated from behind. In this research, at first, frother and collector (because amines may act as a frother) were added to the water of the cell and then the viewing chamber was filled with water of the cell to prevent bubble coalescence [22].

Jg was calculated using air flow rate and area cross section of the cell with the consideration area occupied by the impeller shaft.

The specific input power (P) was inferred from electrical measurements and measuring entrance amperage and voltage to the electrical motor of the flotation equipment.

THEORICAL SECTION

Numerous investigations have shown that with free turbulence the macro scale is of the order of the dimensions of the turbulence-generating systems and normal to the direction of the flow. The structure and intensity of the largest vortices, which are also referred to as macro turbulence, are responsible for the exchange of bulk areas, the so-called eddies between adjacent layers. Thus they determine the turbulent shear stresses and the turbulent transport of mass. The intensity and the structure of the micro turbulence depend only on the magnitude of energy flux and the viscosity of the fluid. The energy flux is equal to the dissipation, i.e., the power per unit mass of fluid which is withdrawn from the basic flow and transformed into heat by the deceleration of the smallest vortices [23]. The mean dissipation in a stirrer, with a power input, P, and a liquid mass, m, is [10]:

$$\varepsilon = P/m \tag{2}$$

The micro scale turbulence, λ_0, is calculated by the following equation [10]:

Table 1: Flotation tests conditions.

Gas Flow Rate (l/hr)	60				120				180				240			
Impeller Speed (rpm)	900	1000	1100	1200	900	1000	1100	1200	900	1000	1100	1200	900	1000	1100	1200
d_b (μm)	830	750	690	630	830	750	680	620	820	750	680	620	820	750	680	620
ε_g (%)	2.86	3.75	4.75	5.87	3.62	4.71	5.93	7.30	4.08	5.29	6.65	8.17	4.48	5.79	7.27	8.92
J_g (cm/s)	0.1	0.1	0.1	0.1	0.2	0.2	0.2	0.2	0.3	0.3	0.3	0.3	0.4	0.4	0.4	0.4
S_b (1/s)	10.21	10.88	11.53	12.16	16.77	17.94	19.08	20.19	22.69	24.31	25.89	27.43	28.23	30.28	32.27	34.2
Re_b	307	229	174	133	303	226	171	131	301	224	170	130	299	223	169	130
ε (W/kg)	2.15	2.95	4.18	5.98	2.15	2.95	4.18	5.98	2.15	2.95	4.18	5.98	2.15	2.95	4.18	5.98
λ_0 (μm)	162	150	137	125	162	150	137	125	162	150	137	125	162	150	137	125

$$\lambda_0 = \left(\frac{\nu^3}{\varepsilon}\right)^{1/4} \tag{3}$$

Where, ν is kinematic viscosity. There is a boundary layer between particles and fluids, the state of which varies with the Reynolds number of the particle because of the motion between the particle and fluid. Also, the boundary layer around the bubble has a critical role in flotation efficiency and capture of particles with bubbles [24].

According to the authors' knowledge, this study is the first attempt at describing the k-S_b relationship using boundary layer around the particles. The particle Reynolds number is given by [25]:

$$Re_p = \frac{d_p u_s}{\nu} \tag{4}$$

Where u_s is the rate of sliding motion of the particle, which can be obtained by the settling rate of particles. When $Re_p < 1$, a boundary layer with laminar flow is
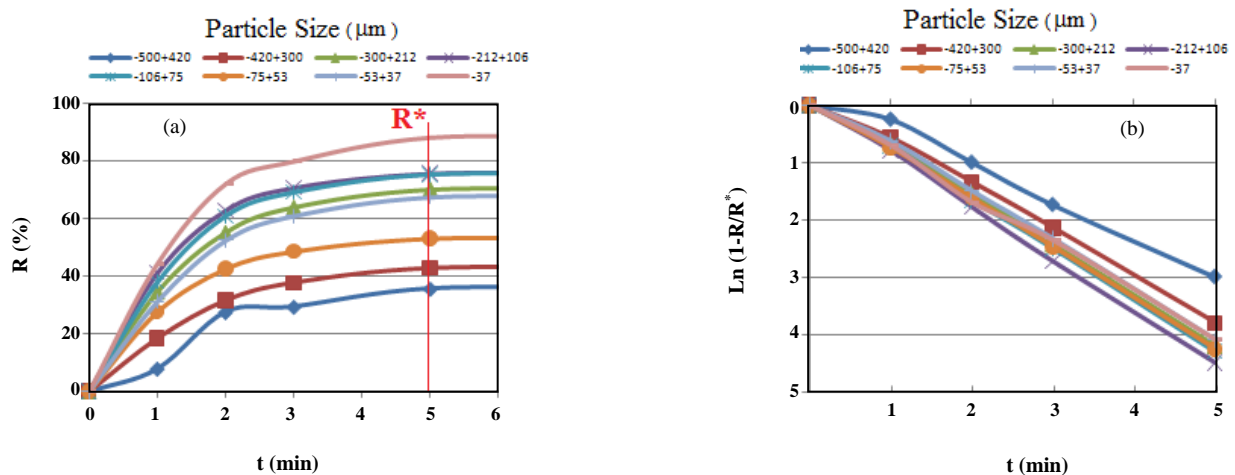
Fig. 1: Calculation of flotation rate constant (k) base on R* for S_b = 28.23 1/s.

formed between the particle and fluid. When $Re_p > 1$, whatever Reynolds number is receded from 1, the flow condition becomes more turbulent. When $Re_p > 10$, the boundary layer breaks off. The flow lines near the coarse particle will curl up to form definite vortices. In this case, part of the kinetic energy of the particle motion is released in the form of heat owing to friction, and the rest of the kinetic energy is turned into work done producing turbulent waves. That is to say, the particles in motion will consume part of the turbulent energy, the other part of which will be consumed by turning big-sized vortices into small-sized vortices, bringing about changes in the frequency spectrum of turbulent motion. The eddy produced by the coarse particle tailing trace is favorable for the aggregation of fine particles. This is the so-called ''promoting aggregation action of coarse particles'', which can be accessed using the particle Reynolds number [25].

The bubble Reynolds number is another hydrodynamic parameter that can influence the flotation rate constant. The bubble Reynolds number is calculated using Eq. (5) [23]:

$$Re_b = V_b d_{32} \rho / \eta \qquad (5)$$

in which, V_b is bubble raise velocity, η is fluid dynamic viscosity and ρ is fluid density.

Also, understanding the various micro processes involved in the collection of solid particles by air bubbles, namely collision, attachment and detachment, is a fundamental step toward predicting the flotation rate

constant [10, 26-28]. The probability of adhesion determines the selectivity of a flotation process, while its recovery depends critically on the collision probability. The flotation rate constant is proportional to the collection efficiency [29], this equation can be seen in the form of the equation below [30]:

$$E_{col} = E_c E_a (1 - E_d) \qquad (6)$$

Where E_c is the collision efficiency, E_a is the attachment efficiency and E_d is the detachment efficiency. The particles are inertia less and therefore follow the streamlines of the fluid, whilst their trajectories can be characterized by the stream function of the fluid. These assumptions imply that collision can occur evenly over the upper half of the bubble. Under the Stokes stream function, the collision efficiency is given by Eq. (7) which is identical to the Gaudin collision model [31,32]:

$$E_c = \frac{3}{2} (d_p / d_b)^2 \qquad (7)$$

Where d_p and d_b are particle and bubble diameter, respectively.

RESULTS AND DISCUSSION
Results
k-S_b Relationship

According to Fig. 2, the flotation rate constant increased with increasing bubble surface area flux and decreasing particle size. Thus, for a bubble surface area
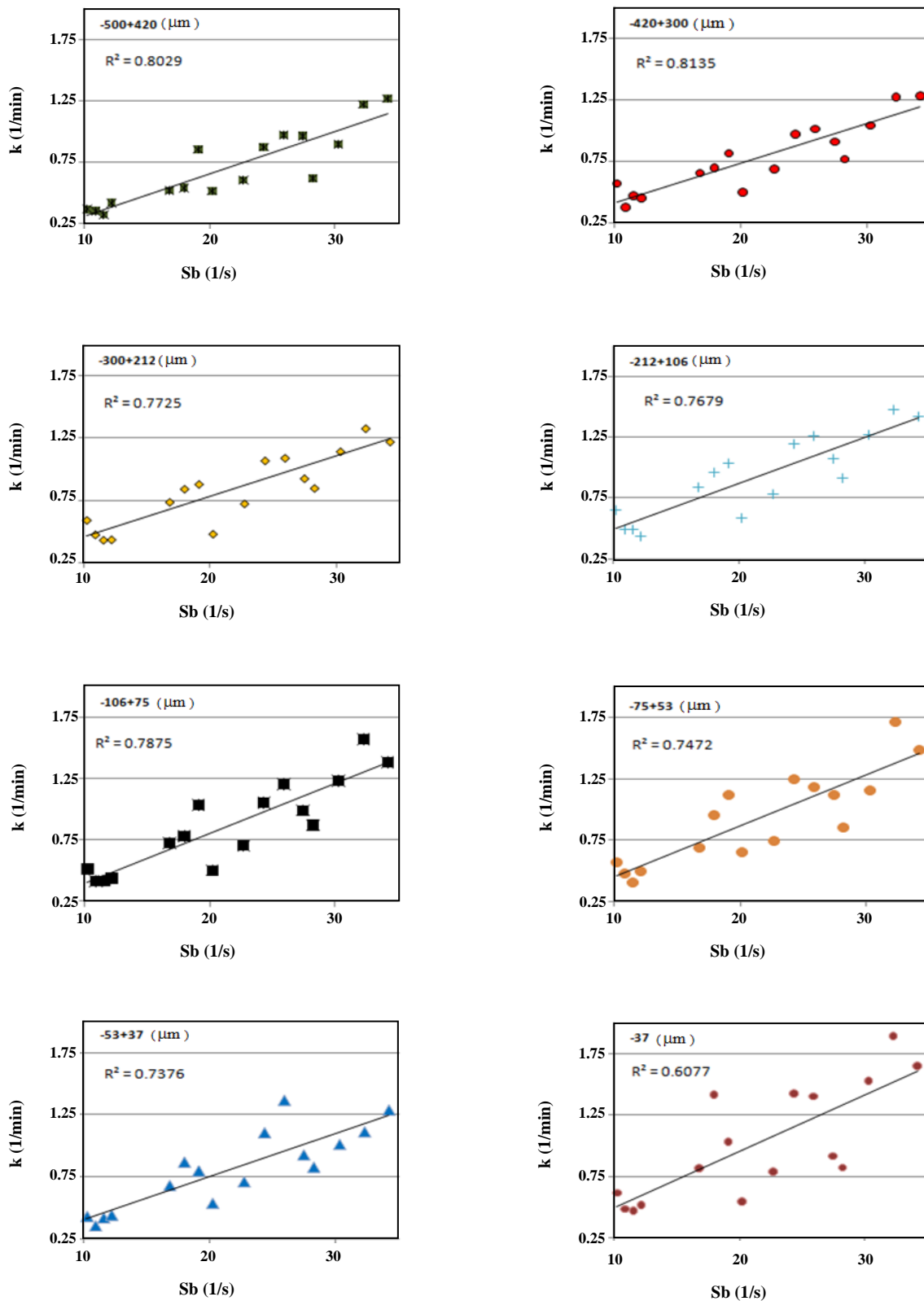
Fig. 2: k-S$_b$ relationship for different particle sizes.

Table 2: Regression statistics for estimating input power.

Multiple R	0.924857953
R Square	0.855362233
Adjusted R Square	0.853772807
Standard Error	5.345473667
Observations	93

Table 3: ANOVA for estimating input power.

	df	SS	MS	F	Significance F
Regression	1	15377.37	15377.37	538.2	5.59E-40
Residual	91	2600.242	28.57409	-	-
Total	92	17977.61	-	-	-
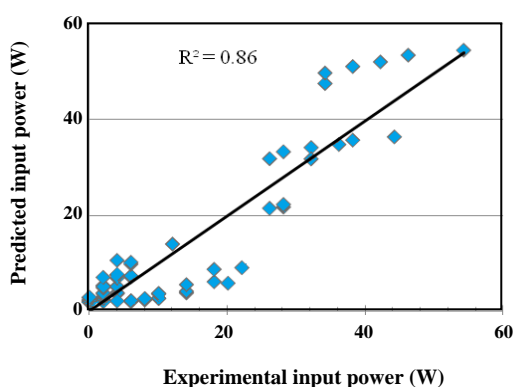
Fig. 3: Experimental P versus Predicted P obtained by Eq. (8).

flux of 28.23 1/s, when the particle size decreases from -500+420 to -37 μm, the flotation rate constant increases from 0.62 to 0.82 1/min. When particle size, impeller speed and bubble surface area flux were -37 μm, 1100 rpm and 32.27 1/s respectively, the maximum flotation rate constant was obtained at 1.89 1/min. Furthermore, when particle size, impeller speed and bubble surface area flux were -500+420 μm, 1100 rpm and 11.53 1/s respectively, the minimum flotation rate constant was obtained at 0.32 1/min.

Input power

Typical mean energy dissipation values in industrial flotation cells range from 1.0 to 5.0 W/kg, depending on the cell size, installed motor power, transmission losses, and slurry density [33]. It is well recognized that energy dissipation is a local function, and also the maximum value

near the impeller may be higher than the mean energy dissipation across the entire cell (10–20 times higher) [34]. In a mechanical flotation cell, the input power may be assumed to be dependent on impeller peripheral speed, superficial gas velocity (neglect able) and pulp density.

In this study, input power was estimated in a laboratory flotation cell. Impeller peripheral speed and pulp density were selected for estimating input power. Different forms of multiple regression models (exponential, linear, polynomial and power) were examined by comparing their statistical significance using the coefficient of multiple determinations (R^2). The final form of the model is shown according to the equation below:

$$P = 0.003 N_s^{5.25} . P_d^{0.07} \qquad R^2 = 0.86 \qquad (8)$$

Where P is input power (watt), N_s is impeller peripheral speed (m/s) and P_d is pulp density (%). The most effective parameter on input power was N_s and the effect of P_d on input power was very low. For $1.83 < N_s < 6.12$ m/s and $0 < P_d < 40\%$, input power was obtained as $0.05 < P < 52.58$ watt. Fig. 3 shows a plot of the predicted values of P from the model versus the experimentally observed values of P. Regression Statistics, ANOVA and Significance of Coefficients have been given in Tables 2 to 4, respectively.

Discussion

Increasing the flotation rate constant with decreasing particle size suggests that the floatability demands some turbulence to promote particle-bubble collision, but that turbulence may not be high enough to destroy particle-

Table 4: Significance of coefficients for estimating input power.

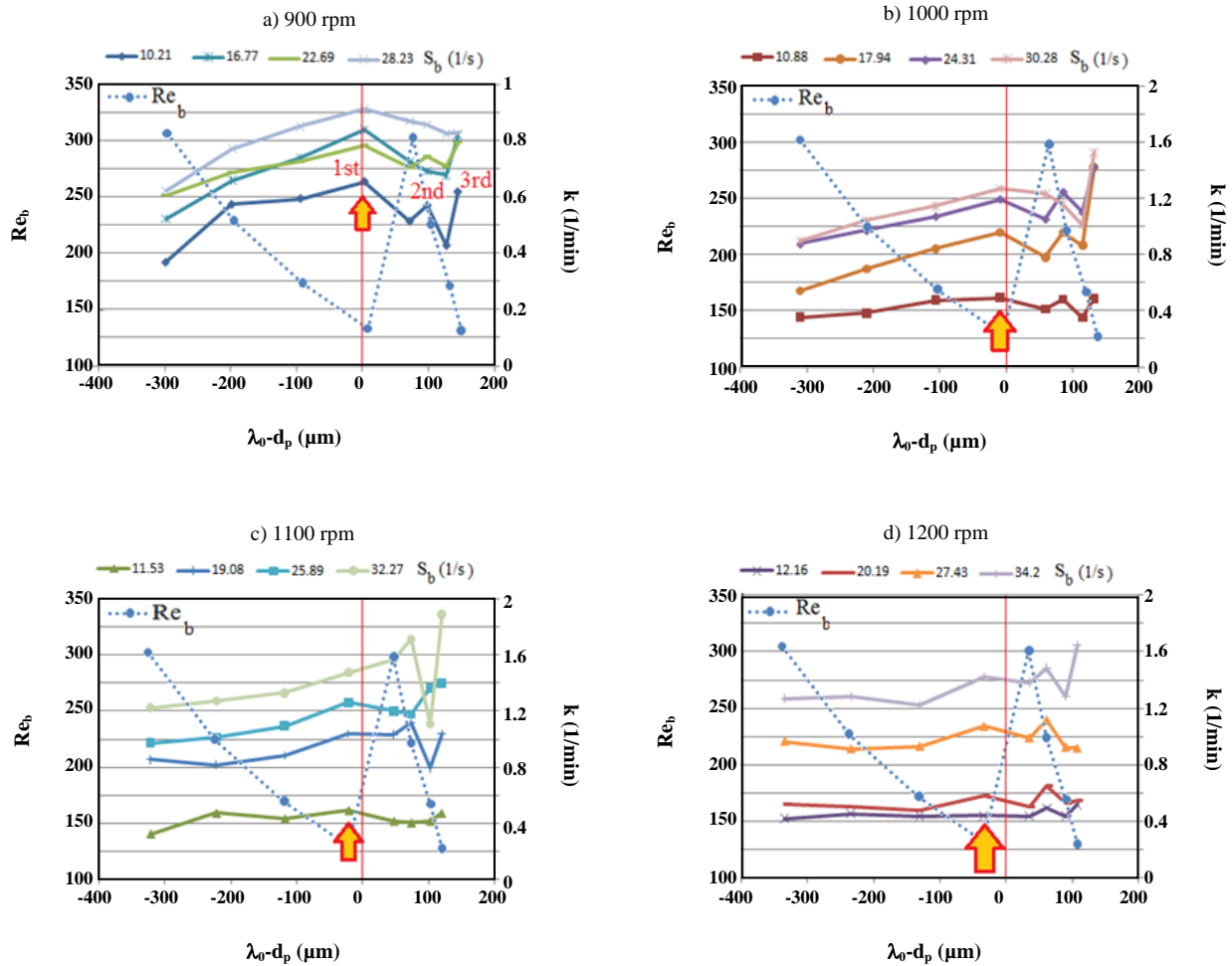|	Coefficients	Standard Error	t Stat	P-value	Lower 95%	Upper 95%
Intercept	8.11211E-08	0.702873	1.15E-07	1	-1.39617	1.396171
X Variable 1	0.995459211	0.042911	23.19823	6E-40	0.910222	1.080697

Fig. 4: The Effect of micro turbulence and bubble Reynolds number on the k-S_b relationship.

bubble aggregates. Also, coarser quartz particles showed a pronounced lower flotation rate than finer ones. It seems that bigger particles demand much more turbulence to become suspended and collide with air bubbles than smaller ones.

Impeller speed is an influence parameter on input power and micro scale turbulence. The k-S_b relationship at different impeller speeds has been shown in Fig. 4. It can be seen that when λ_0-d_p > 0, i.e. the size of the particles is less than the turbulent micro scale, λ_0, the flotation rate constant rising and falling with no consistent pattern. When λ_0-d_p > 0, i.e. the particle size is greater than λ_0, the flotation rate constant decreases with the increase of particle size. This shows that an optimal particle size, $\lambda_0 = d_p$, exists for coarse particles. Using the particles with a size of $\lambda_0 = d_p$, the flotation rate constant of coarse particles reaches a maximum. In this research, the maximum flotation rate for coarse particles was obtained at 1.47 1/min, with bubble surface area flux of 32.27 1/s and impeller speed of 1100 rpm.

In this research, the bubble Reynolds number was obtained from 130 to 307. Fig. 5 shows bubble Reynolds
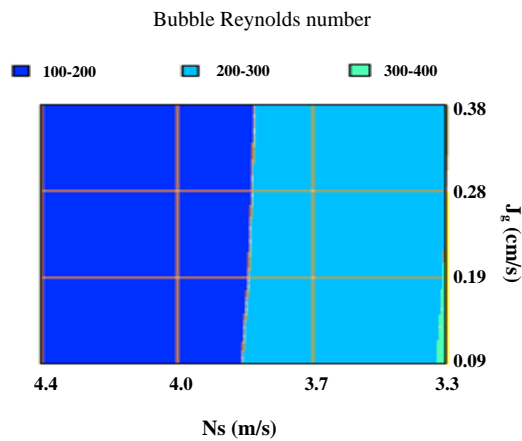
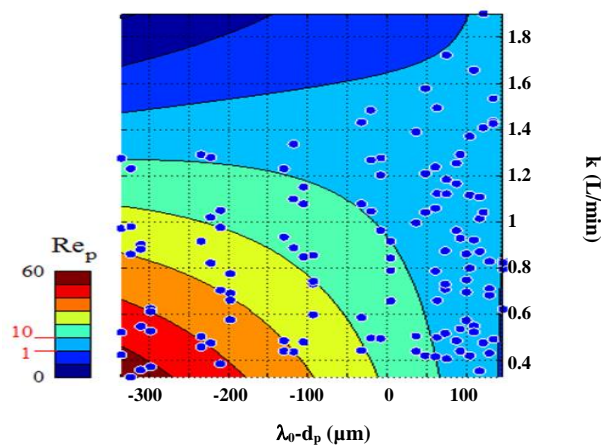**Fig. 5: Bubble Reynolds number in different peripheral impeller speeds and superficial gas velocity.**

Fig. 6: Particle Reynolds number in different conditions (blue circles are experimental data).
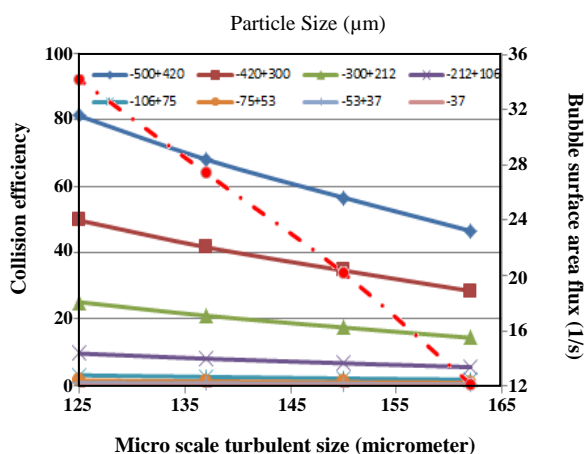

Fig. 7: The effect of micro scale turbulence size on collision efficiency (air flow rate of 240 l/h).

numbers for different peripheral impeller speeds (N_s) and superficial gas velocity (J_g). According to Fig. 4, a plateau of maximum flotation rate was obtained by a bubble Reynolds number of 170 and with increasing bubble Reynolds numbers, the flotation rate decreased. When the bubble Reynolds number was 307, the flotation rate of all particle sizes decreased.

Also, the particle Reynolds number was estimated for a different particle size, flotation rate and micro turbulent size and Eq. (9) was obtained. Different forms of multiple regression models (exponential, linear, polynomial and power) were examined by comparing their statistical significance using a coefficient of multiple determinations (R^2). Estimation of Re_p has been shown in Fig. 6.

$$Re_p = 13.49 - 6.282k - 10.45(\lambda_0 - d_p) + \qquad (9)$$

$$5.743k(\lambda_0 - d_p) - 0.961(\lambda_0 - d_p)^2$$

$$R^2 = 0.98$$

So, the particle Reynolds number was calculated for different conditions and the maximum particle Reynolds number was obtained at 60.25 with a particle size of 460 μm, impeller speed of 900 rpm, bubble surface area flux of 10.21 1/s and micro scale turbulence size of 162 μm.

The effect of micro scale turbulence size on collision efficiency was investigated using Eq. (7). Variations of Stokes collision efficiency with particle size has been shown in Fig. 7. The Stokes collision efficiency was calculated for different particle sizes ($0.07 < E_c < 81.89\%$). Maximum Stokes collision efficiency was obtained 81.89% with micro scale turbulence size of 125 μm, bubble surface area flux of 34.2 1/s and particle size of -500+420 μm and in this condition the flotation rate constant was obtained 1.27 1/min. Minimum collision efficiency was obtained 0.07% with micro scale turbulence size of 162 μm, particles size of -37 μm and bubble surface area flux of 10.21 1/min. So, bubble-particle collision efficiency increased with decreasing micro scale turbulence size.

According to Fig. 8, the Reynolds number of coarse particles (-500+420, -420+300, -300+212 and -212+106 μm) was more than 10. In these conditions, the flotation rate constant was increased with the decreasing particle Reynolds number. Maximum flotation rate constant (1st peak) was obtained with $\lambda_0 = d_p$. The Reynolds number of medium particles (-106+75, -75+53 and -53+37 μm) was
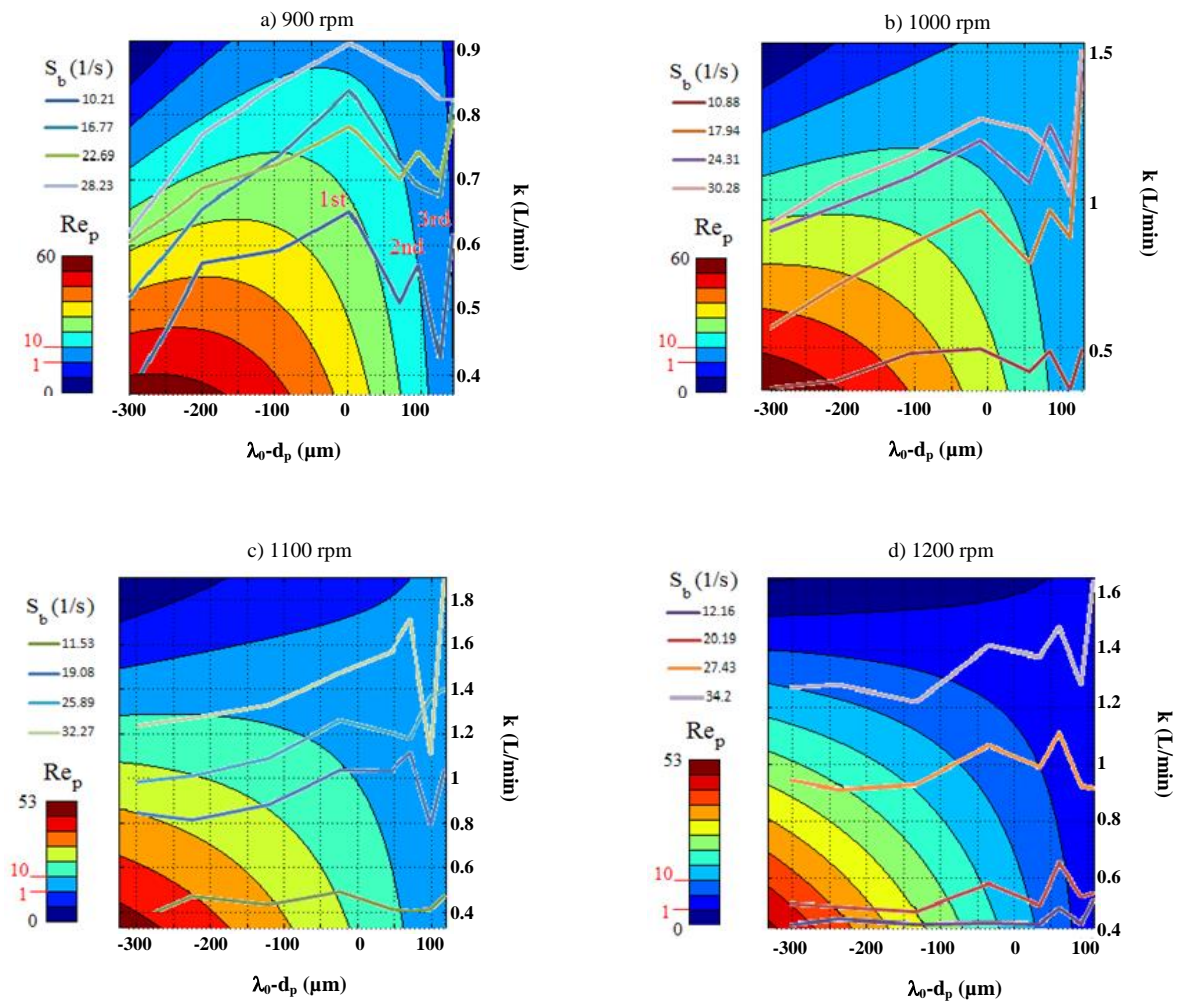
Fig. 8: The effect of particle Reynolds number on the k-S_b relationship.

between 1 and 10. In these conditions, a maximum flotation rate constant (2nd peak) was obtained with a particle size of -75+53 μm. The Reynolds number of fine particles (-37 μm) was less than 1. In these conditions, the flotation rate constant increased sharply and the 3rd peak was obtained.

CONCLUSIONS

In this research, the effect of input power and micro turbulence on the k-S_b relationship was investigated and the following conclusion was obtained:

- When particle size, impeller speed and bubble surface area flux were -37 μm, 1100 rpm and 32.27 1/s, respectively, a maximum flotation rate constant was obtained at 1.89 1/min.

- The most effective parameter on input power was N_s

and the effect of P_d on input power was very low. For $1.83 < N_s < 6.12$ m/s and $0 < P_d < 40\%$, input power was obtained at $0.05 < P < 52.58$W.

- When $\lambda_0 - d_p < 0$, i.e. the particle size is greater than the λ_0, the flotation rate constant decreases with the increase of particle size. This shows that an optimal particle size, $\lambda_0 = d_p$, exists for coarse particles.

- A plateau of maximum flotation rate constant was obtained by a bubble Reynolds number of 170 and with increasing bubble Reynolds numbers, the flotation rate constant decreased.

- The maximum particle Reynolds number was obtained at 60.25 with a particle size of -500+420 μm, impeller speed of 900 rpm, bubble surface area flux of 10.21 1/s, and micro scale turbulence size of 162 μm.

REFERENCES

[1] Gorain B.K., Franzidis J.P., Manlapig E.V., Studies on Impeller Type, Impeller Speed and Air Flow Rate in an Industrial Scale Flotation Cell. Part 4: Effect of Bubble Surface Area Flux on Flotation Performance, *Minerals Engineering*, **10:** 367-379 (1997).

[2] Hernandez H., Gomez C.O., Finch J.A., A Test of the Flotation Rate vs. Bubble Surface Area Flux Relationship, J.A. Finch, S.R. Rao, L. Huang (Eds.), "Proceedings of 4th UBC-McGill Symposium on Fundamentals in Mineral Processing, Toronto", August 26–29, 59-74 (2001).

[3] Hernandez H., Gomez C.O., Finch J.A., Gas Dispersion and Deinking in a Flotation Column, *Minerals Engineering*, **16**: 739-744 (2003).

[4] Hernandez-Aguilar, J.R., Rao, S.R., Finch, J.A., Testing the k-Sb Relationship at the Micro Scale, *Minerals Engineering*, **18**: 591-598 (2005).

[5] Gorain B.K., Napier-Munn T.J., Franzidis J.P., Manlapig E.V., Studies on Impeller Type, Impeller Speed and Air Flow Rate in an Industrial Scale Flotation Cell. Part 5: Validation of k-Sb Relationship and Effect of Froth Depth, *Minerals Engineering*, **11**: 615-626 (1998).

[6] Pyke B., "Bubble-Particle Capture in Turbulent Flotation Systems", Ph.D. Thesis, University of South Australia, Australia, (2003).

[7] Pyke B., Fornasiero D., Ralston J., Bubble Particle Heterocoagulation Under Turbulent Conditions, *Journal of Colloid Inputface Science*, **265**: 141–151 (2003).

[8] Bloom F., Heindel T.J., On the Structure of Collision and Detachment Frequencies in Flotation Models, *Chemical Engineering Science*, **57**: 2467–2473 (2002).

[9] Schubert H., Die Modellierung des Flotations Prozesses auf Hydrodynamischer, *Grundlage-Neue Bergbautechnik*, **7**: 446-456 (1977).

[10] Schulze H.J., "Physico-Chemical Elementary Processes in Flotation: An Analysis from the Point of View of Colloid Science Including Processes Engineering Considerations", Dev. in Mineral Processing, (Fuerstenau, D.W., Advisory Ed.), Elsevier, Amsterdam, **4**: 348 (1984).

[11] Chehreh Chelgani S., Shahbazi B., Rezai B., Estimation of Froth Flotation Recovery and Collision Probability Based on Operational Parameters Using an Artificial Neural Network, *International Journal of Minerals, Metallurgy and Materials*, **17**: 526-534 (2010).

[12] Shahbazi B., Rezai B., Koleini Javad S.M., Effect of Dimensionless Hydrodynamic Parameters on Coarse Particles Flotation, *Asian Journal of Chemistry*, **3**: 2180-2188 (2008).

[13] Shahbazi B., Rezai B., The Effect of Type and Dosage of Frothers on Coarse Particles Flotation, *Iran. J. Chem. Chem. Eng. (IJCCE)*, **28**: 95-101 (2009).

[14] Shahbazi, B., Rezai, B., Koleini, S.M. Javad, Noaparast M., The Effect of Dimensionless Parameters on Coal Flotation, *International Journal of Coal Preparation and Utilization*, **32**: 157-168 (2012).

[15] Shahbazi B., Rezai B., Koleini S.M. Javad, Noaparast M., The Effect of Bubble Surface Area Flux on Flotation Efficiency of Pyrite Particles, *Iran. J. Chem. Chem. Eng. (IJCCE)*, **32**: 109-118 (2013).

[16] Shahbazi B., Rezai B., Koleini S.M.J., Noaparast M., The Study of Influence of Bubble Surface Area Flux on Flotation Rate Constant of Coal Particles, *Geosciences*, **23**: 45-52 (2014).

[17] Shahbazi B., Rezai B., The Effect of Dimensionless Parameters and Bubble Surface Area Flux on Flotation Rate Constant, *Journal of Dispersion Science and Technology*, **36**: 471-476 (2015).

[18] Shahbazi B., Rezai B., Chehreh Chelgani S., Koleini S.M.J., Noaparast M., Estimation of Diameter and Surface Area Flux of Bubbles Based on Operational Gas Dispersion Parameters by Using Regression and ANFIS, *International Journal of Mining Science and Technology,* **23**: 343-348 (2013).

[19] Shahbazi B., Rezai B., Koleini S.M.J., Noaparast M., Estimation of Gas Holdup and Input Power in Froth Flotation Using Artificial Neural Network, *Iranian Journal of Materials Science and Engineering*, **12**: 12-20 (2015).

[20] Ehsani M.R., Eghbali F., Reduction of Sulfur and Ash from Tabas Coal by Froth Flotation, *Iran. J. Chem. Chem. Eng. (IJCCE)*, **26**: 35-40 (2007).

[21] Ahmadi R., Khodadadi Darban A., Abdollahy M., Flotation of Chalcopyrite Fine Particles in the Presence of Hydrodynamic Cavitation Nano Bubbles, *Nashrieh Shimi va Mohandesi Shimi Iran*, **32**: 81-91(2013). [In Persian]

[22] Girgin E.H., Do S., Gomez C.O., Finch J.A., Bubble Size as a Function of Impeller Speed in a Self-Aeration Laboratory Flotation Cell, *Minerals Engineering*, **19**: 201-203 (2006).

[23] Ralston J., Fornasiero D., Hayes R., Bubble-Particle Attachment and Detachment in Flotation, *International Journal of Mineral Processing*, **56**: 133-164 (1999).

[24] Dukhin S.S., Miller R., Loglio G., Physico-Chemical Hydrodynamic of Rising Bubble, "Drops and Bubbles in Interfacial Research", D. Mobius and R. Miller (Editors) Elsevier Science B.V. All rights reserved, (1998).

[25] Hu Yuehua, Qiu, Guangzhou, Miller J.D., Hydrodynamic Interactions Between Particles in Aggregation and Flotation, *Int. J. Miner. Process*, **70**: 157– 170 (2003).

[26] Dobby G.S., Finch J.A., Particle Size Dependence in Flotation Derived from a Fundamental Model of the Capture Process, *Int. J. Miner. Process*, **27**: 241-263 (1987).

[27] Crawford R., Ralston J., The Influence of Particle Size and Contact Angle in Mineral Flotation, *Int. J. Miner. Process*, **23**: 1-24 (1988).

[28] Hewitt D., Fornasiero D., Ralston J., Bubble-Particle Attachment, *J. Chem. Soc. Faraday Trans*, **13**: 1997-2001 (1995).

[29] Jameson G.J., Nam S., Young M.M., Physical Factors Affecting Recovery Rates in Flotation, *Min. Sci. Eng*, **9**: 103-118 (1977).

[30] Schulz, H.J., Hydrodynamics of Bubble-Mineral particle collisions, *Min. Process. Extractive. Metall*, **5**: 43-76 (1989).

[31] Dai Z., Fornasiero D., Ralston J., Particle-Bubble Collision Models-A Review, *Adv. Colloid. Interfac*, **85**: 231-256 (2000).

[32] Yoon R.H., The role of Hydrodynamic and Surface Forces in Bubble-Particle Interaction, *Int. J. Miner. Process*, **58**: 129-143 (2000).

[33] Deglon D.A., Egya-mensah D., Franzidis J.P., Review of Hydrodynamics and Gas Dispersion in Flotation Cells on South African Platinum Concentrators, *Minerals Engineering*, **13**: 235-244 (2000).

[34] Schubert H., On the Turbulence-Controlled Micro Processes in Flotation Machines, *International Journal of Mineral Processing*, **56**: 257-276 (1999).